EVS24
Stavanger, Norway, May 13-16, 2009

Integrated Control of Anti-lock Braking with Regenerative Braking

Zhang Junzhi, Zhang Pengjun, Chen Xin and Lu Xin
Dept. Automotive Engineering, Tsinghua University, jzhzhang@mail.tsinghua.edu.cn

Abstract

This paper mainly focuses on the integrated control of an HEV's brake system, especially the integration of the friction braking and the regenerative braking during anti-lock braking control. Based on a series regenerative braking system, the structure of an integrated brake system is proposed. The models of each part of a hybrid electric bus are built in Matlab/Simulink taking authorized articles as references. A test bench with the original pneumatic brake system of a bus is also built to carry out hardware-in-the-loop test (HIL test) of the integrated brake system and to study the characteristic of the system better. The integrated control strategy is proposed based on pneumatic anti-lock braking strategy. Simulation results show that the participation of regenerative braking in the anti-lock braking control can be beneficial to both the riding comfort and the braking performance of the vehicle. HIL test results validates the results of the simulations. The field in which further research could be carried out is also proposed.

Keywords: HEV, regenerative braking, anti-lock braking, simulation, hardware-in-loop test

1 Introduction

Studies show that in urban driving about one third to half of the energy of power plant is consumed during brake [1][2]. As regenerative braking can improve the fuel economy effectively, the hybrid electric vehicle with internal combustion engine (HEV for short) usually takes regenerative braking as the threshold of its concept. A vehicle featuring idle-off but no regenerative braking is commonly not considered as an HEV [3]. It is claimed that vehicle fuel economy can be enhanced by up to 15% through the application of regenerative braking [4].

Regenerative braking control strategies can be sorted as series or parallel. The parallel strategy exerts the braking torque of the electric motor via transmission on the wheels without interfering the frictional braking torque. The series strategy exerts the regenerative braking torque and modulates the frictional braking torque, targeting at giving out a certain overall braking torque according to the stroke of the braking pedal. Thus the series strategy for regenerative braking is also called the strategy of 'brake blending' [5]. It is obvious that under series strategy more braking energy can be recaptured. Due to the flexibility and the better capacity of regenerating braking energy, more and more HEVs adopt series regenerative braking strategy. For example from 2006 the Honda Civic hybrid began to feature blending of the frictional and regenerative braking [6].

Meanwhile the anti-lock braking system has long been made a compulsory device on board by legislators around the world. As an example, in 1996 NHTSA amended 'Federal Motor Vehicle Safety Standard 121: Air Brake Systems' to require ABS on all new heavy vehicles [7].

Series regenerative braking and anti-lock braking share a same feature that is the modulation of the frictional brake force. The coordination of the regenerative braking and anti-lock braking and even the integration of the two brakings are of great interest of the automobile manufacturers and institutes. Akihito Kusano of Toyota proposed a brake pressure control device aiming at the integration of regenerative braking and anti-lock braking [8]. Continental Teves has developed an integrated brake system for the Escape hybrid SUV [9]. Honda developed an integrated brake master cylinder to carry out this function [10]. TRW's solution bases on traditional booster-master cylinder and its modulation of braking force is carried out by adjusting the boosting force of the booster [5]. Chu Liang from Jilin University proposed a solution for the coordination of regenerative braking and anti-lock braking based on pneumatic brake system for buses and coaches, though the strategy for regenerative braking is parallel[12].

The author of this article has been dedicated to the research and development of regenerative braking for a couple of years. A series regenerative braking system has been developed and tested on two hybrid buses, namely an HCNG-Hybrid city bus and a fuel cell hybrid city bus[11]. So as to further the research and ensure the braking safety and efficiency of vehicle under both normal deceleration and emergency brakes, the integrated control of regenerative braking and anti-lock braking based on pneumatic brake system has been studied. The topology is based on the already developed brake system with series regenerative braking. The anti-lock braking control strategy takes some open documents as reference and has been proved to function well. In order to facilitate the research, a set of models, including those of the tyre, the vehicle and the pneumatic system, have been built. A pneumatic brake system test bench with pneumatic modulating valves is also built to better simulate a system on board. The integrated system for regenerative braking and anti-lock braking and its strategy have been simulated and hardware-in-the-loop tested. Some results are to be presented in this article.

2 System layout

2.1 Pneumatic brake system with series regenerative braking

In previous research, a regenerative braking system has been developed and applied on vehicles which are rear-wheel-drive serial hybrid buses with pneumatic frictional brakes. Fig.1 is the diagram of the whole system.

Two valves modulate the pneumatic brake force under the control of vehicle controller to cooperate with the regenerative brake force of the electric motor. A separate anti-lock braking system of WABCO is equipped for braking under extreme conditions.

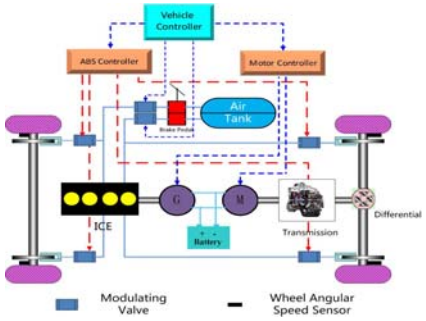

Figure 1: Diagram of the series regenerative braking system

The control strategy is series, taking into consideration of electric bus voltage, battery SOC (state of charge) and the velocity of the vehicle. The system can recapture more than 50% of the braking energy that formerly shall be dissipated by frictional brake wares under some circumstances [11]. It contributes a reduced fuel consumption of 15% on the fuel cell hybrid bus under Chinese City Bus Driving Cycle. The test result of fuel economy is presented in Table 1. A better performance can be expected after further optimization.

2.2 Integrated brake system with regenerative braking and anti-lock braking

There are two sets of pneumatic modulating valves in the regenerative braking system above. One set of valves are in charge of air pressure modulation during normal deceleration (brake blending), the other set of valves belong to the separate ABS as modulators during anti-lock braking control.

There are mainly two disadvantages of the previous system involving regenerative braking and anti-lock braking. First, there is a redundancy of modulators. It is possible to use the same set of valves to carry out the same functions. Second,

Table 1: Effect of the series regenerative braking system

	H_2 consumption by fuel cell stacks kg/100km	Eqv.H2 consumption of battery output kg/100km	Eqv.H2 consumption overall kg/100km
Series regenerative braking	7.18	0.34	7.52
Non-regenerative braking	8.19	0.66	8.85
Fuel consumption reduced by regenerative braking			15.03%

there is a barrier between the two control units, making it difficult to modulate the regenerative braking when anti-lock braking control is in need. Motor torque of regenerative braking can be helpful in anti-lock braking control, which is to be discussed later in this article.

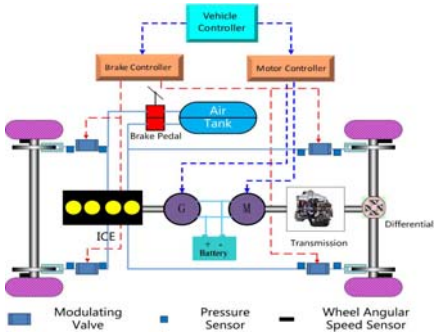

Figure 2 Diagram of the integrated brake system

Fig.2 illustrates the diagram of the proposed integrated brake system with regenerative braking and anti-lock braking. A brake controller takes over the control of all the four modulating valves. It also communicates with the motor controller via vehicle controller to give out a regenerative torque command and receive a motor torque limit. During normal decelerations, the brake controller modulates the pneumatic pressure by controlling the modulating valves while requesting a regenerative torque. Thus the brake blending can be carried out. Wheel speed sensors monitoring the speeds of the four wheels are connected to the brake controller as well. When there is a need of anti-lock braking control by the control strategy, the brake control unit modulates the pneumatic pressure as an ABS controller, meanwhile gives out command of motor torque. The frictional brake and the regenerative brake cooperate with each other to avoid a wheel lock and maintain the stability of the vehicle.

3 Modelling the system

Simulation is a crucial step of research and development nowadays and the model shall be rational to obtain reasonable result. Models of every part of the vehicle including the brake system have been properly built.

3.1 Vehicle dynamics

The research at present mainly focuses on the longitudinal motion of vehicle during braking, but it is obvious that the lateral motion and steering are crucial in research relative to anti-lock braking control. Thus a model of vehicle dynamics with 15 degrees of freedom has been built.

An $O_1X_1Y_1Z_1$ coordinate system is defined first, which is static relative to the space. The origin O_1 coincides with the center of gravity of the vehicle at the beginning of the braking, while the axis O_1X_1 is alongside the longitudinal direction of the vehicle pointing forward. The plane $O_1X_1Y_1$ is parallel to the ground and the axis O_1Z_1 is perpendicular to the ground pointing upward. The $OXYZ$ coordinate system, which adheres to the vehicle, has its origin at the center of gravity of the vehicle. OX is alongside the longitudinal direction of the vehicle pointing forward. Plane OXY is parallel to the ground with OZ perpendicular to the OXY pointing upward. Both coordinate systems are right-handed ones. The yaw angle of the vehicle, the heeling angle of the sprung mass and the pitch angle of the sprung mass are denoted as Y_{aw}, φ and θ respectively whose vectors are alongside the OZ, OX and OY.

The 15 degrees of the vehicle model are namely: displacements of the vehicle along the O_1X_1 and

O_1Y_1 denoted as x and y respectively; vertical motion of the sprung mass of the vehicle along the OZ denoted as z ; The yaw angle, the heeling angle and the pitch angle Yaw, φ and θ; vertical motions of the four wheels z_{FL}, z_{FR}, z_{RL} and z_{RR}; rotations of the four wheels (as rotational speeds) ω_{FL}, ω_{FR}, ω_{RL} and ω_{RR}; steering angle of the front wheels δ.

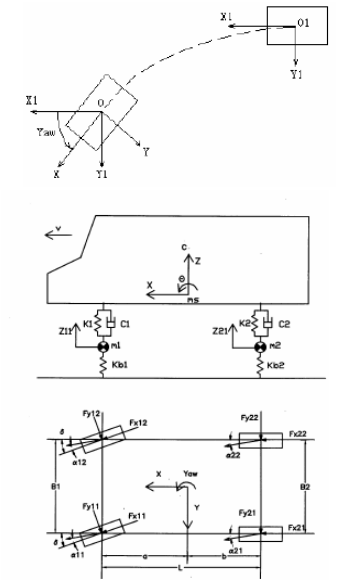

Figure 3 Diagram of the coordinate systems and vehicle model

The parameters of the model come from the data by FOTON which is the manufacturer of the HCNG hybrid city bus.

3.2 Tyre

The tyre model is very important for research on braking, especially on anti-lock braking.

The tyre model proposed by Gwanghun Gim from University of Arizona in [13] is an analytical one. It is capable of simulating the tyre under pure slip ratio, pure slip angle, pure camber angle and the combination of the three. The research on regenerative braking and anti-lock braking focuses mainly on longitudinal motions for the time being. Only pure slip is taken into consideration.

The author of [13] stated that the longitudinal stress may be assumed to depend on the longitudinal stiffness and the longitudinal elastic deformation in the adhesion region and to depend on the contact pressure and the tyre-road friction coefficient in the sliding region.

In [14] the author presented several sets of experimental data, including the slip ratio-longitudinal force curves. The relation between the longitudinal stiffness and the geometric parameters of the tyre is suggested in [15]. Thus, by data extrapolation and geometry calculation, the longitudinal stiffness of the front tyre can be reasonably chosen as 342545N/slip, and that of the rear tyre as 588954N/slip, even if the data of tyre equipped on the HCNG hybrid bus is not available. The characteristic of the longitudinal force of the front wheel on different surfaces is illustrated in Fig.4. The equivalent friction parameter is defined as the ratio of the longitudinal force to the normal force. The equivalent friction parameter is calculated as if there were no load transfer. In actual braking the equivalent friction parameter may differ a little bit at every slip ratio. The characteristic of the rear wheels is similar to the front wheels.

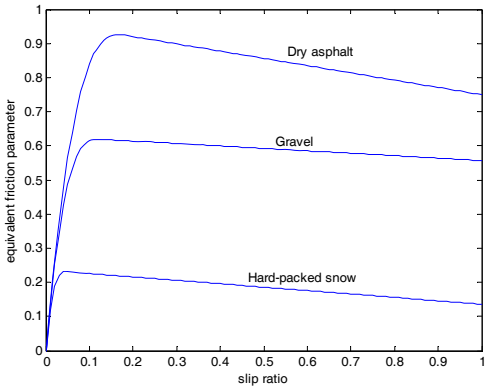

Figure 4 The equivalent friction parameter of the front wheel on different surfaces

3.3 Battery

The battery model is based on the one of the NiMH battery of General Motor EV in ADVISOR. Its original capacity is 60Ah with lock-up tables receiving previous SOC and temperature and giving out charging/discharging internal resistance of the battery. The look-up tables are updated with data from General Research Institute for Nonferrous Metals of China, which is the manufacturer of the 80Ah NiMH battery equipped on the HCNG. The model's input is the power requested by the electric motor. Its output includes the SOC, the voltage at the output port of battery, the current and the temperature of the battery.

3.4 Electric motor

The model of the electric motor has been built according to the data from the supplier and some test results.

The electric motors equipped on the HCNG hybrid bus and the fuel cell hybrid bus are products of the Zhuzhou Electric Locomotive Research Institute. The overall efficiency of the motor system including the electric motor and its controller while driving is illustrated as an efficiency map in Figure 5. The outer characteristic of the electric motor system is also shown in the figure. The efficiency map in the regenerative braking mode is almost symmetrical to that in driving mode with respect to the axis of rotational speed.

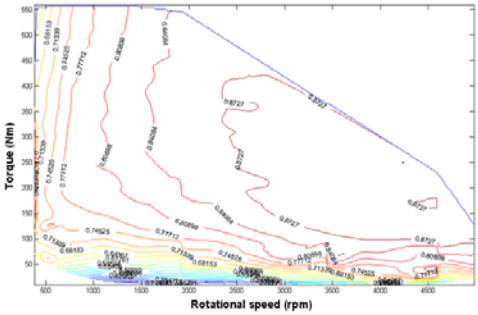

Figure 5 Efficiency map of the electric motor system

The electric motor and its controller are so tuned that the output torque of the motor covers 95% of the change in required torque in approximately 0.6s. Thus the electric motor system can be expressed as lag tache and the efficiency map.

3.5 Pneumatic system

In [16] the author proposed a model for the pneumatic subsystem of an S-cam air brake system, which is of the same type of brake equipped on the HCNG hybrid bus. The model was built taking in to consideration of the dynamics of the treadle valve, the dynamics of the brake chamber, and the flow of air in the system. In the article the author not only built the model of the pneumatic system, but also corroborated it with experiment. The model was able to simulate the system properly. The author provided the parameters of the pneumatic system as well. The size of the brake chamber, the radius of the pipe and the working pressure are the same as the pneumatic brake system equipped on the HCNG hybrid bus. So it is rational to apply the same model when simulating the pneumatic subsystem in the integrated brake system.

When studying the integrated control of the regenerative braking and the anti-lock braking, the flow of air and the motion of the piston propelled by the brake chamber are of most interest. Thus the airflow part and the brake chamber part take [16] as reference. The author stated that for various test runs the value of the Mach number was found not to exceed 0.2 ensuring that the effects of compressibility of air for the flow through the hose can be neglected.

a governing equation for the pressure transients in the brake chamber during the apply phase with the term P_o being the supply pressure can be obtained as (1).

$$\left(\left(\frac{2\gamma}{\gamma-1}\right)\frac{1}{RT_o}\left|\left[\left(\frac{P_b}{P_o}\right)^{(2/\gamma)}-\left(\frac{P_b}{P_o}\right)^{((\gamma+1)/\gamma)}\right]\right|\right)^{1/2}A_pC_DP_o\,\mathrm{sgn}(P_o-P_b)] \quad (1)$$

$$=\begin{cases}\left(\frac{V_{o1}P_o^{((\gamma-1)/\gamma)}}{\gamma RT_oP_b^{((\gamma-1)/\gamma)}}\right)\dot{P}_b & if \quad P_b<P_t\\ \left(\frac{V_bP_o^{((\gamma-1)/\gamma)}}{\gamma RT_b}+\frac{P_b^{1/\gamma}A_b^2P_o^{((\gamma-1)/\gamma)}}{RT_bK_b}\right)\dot{P}_b & if \quad 0<x_b<x_{b\max}\\ \left(\frac{V_{o2}P_o^{((\gamma-1)/\gamma)}}{\gamma RT_oP_b^{((\gamma-1)/\gamma)}}\right)\dot{P}_b & if \quad x_b=x_{b\max}\end{cases}$$

In equation (1), P_b is the local pressure inside the control volume, V_{o1} is the initial volume of air in the control volume before the application of the brake, V_{o2} is the maximum volume of air in the control volume, V_b is the volume of the control volume, A_b is the cross-sectional area of the brake chamber, x_b is the stroke of the brake chamber diaphragm, i.e., the stroke of the push rod, $x_{b\max}$ is the maximum stroke of the push rod and P_t is the 'push-out' pressure. $P_b<P_t$ corresponds to the phase when x_b =0. T_b is the local temperature inside the control volume at that instant of time. R is the gas constant for air. γ is the ratio of the specific heats.

Most of the parameters in the pneumatic subsystem model are identical to those in reference [16]. However some of them, including the discharge coefficient C_D is redefined by experiment on the hardware-in-the-loop test bench which will be introduced later in this article.

The friction brake torque is assumed to be applied on the drum when the pushing rod is fully push out i.e. when x_b equals $x_{b\max}$. The pneumatic pressure

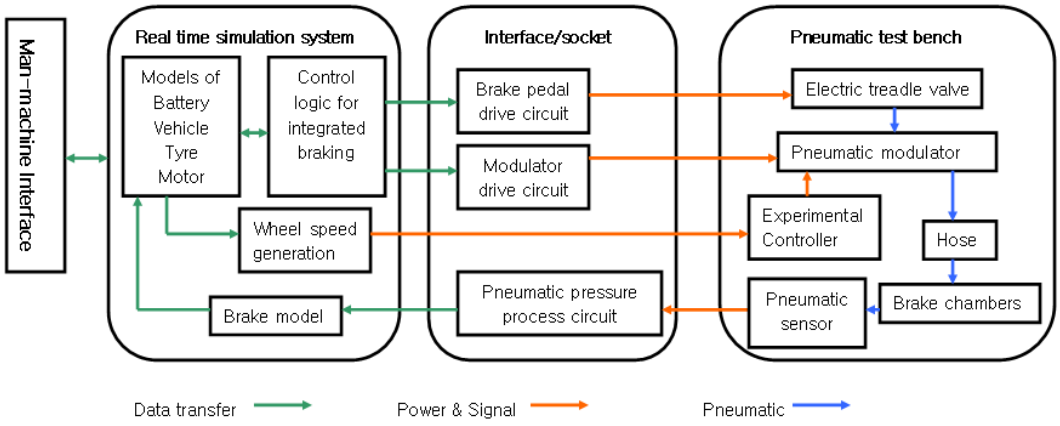

Figure 7. The configuration of the integrated brake system test system

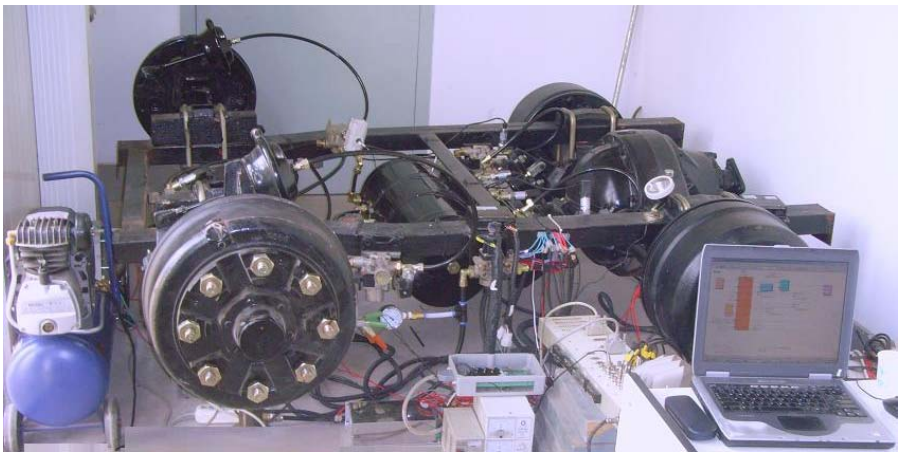

Figure 8 Test system for integrated brake control

to brake torque ratio K_{pb} is acquired during brake testing of the HCNG hybrid bus.

$$Trq_b = K_{pb} P_b \quad (2)$$

Trq_b is the friction brake torque applied on the wheel. P_b is the pneumatic pressure in the brake chamber.

On the front axle the ratio is 1258.2Nm/bar for a single wheel brake ware. On the rear axle the ratio is 1793.3Nm/bar for a single wheel brake ware.

4 Experiment setup

The models of the subsystems within the integrated brake system can be rational to simulate the real system well. However it is still a better way of research to replace the virtual models with real components and carry out hardware-in-the-loop tests.

Of all the models mentioned in the previous part, the one of pneumatic system is complex and hard to resemble the real system much. Figure 7 illustrates the configuration of the test system for integrated brake system. The pneumatic system including the compressor, the air reservoir, the pneumatic modulating valves and the brake chambers is the same as that equipped on board. The test system is comprised of the real time simulation system, the interface/socket and the pneumatic test bench. The real time simulation system is an 'Auto box' manufactured by DSpace, with a DS1005 processor board and a DS2211 I/O board. The control logic for integrated braking can be included in the 'Auto box' or the experimental controller which is to be equipped on the vehicle. Thus the test system is able to cover several phases of R&D, from the control logic prototyping to the calibration and test of the control unit. Figure 8 is a picture of the test system.

5 Control strategy

The integrated control strategy is composed of the strategy on normal braking conditions (no wheel is locked or to be locked) and the strategy during anti-lock braking control. The former part including the discussion of different brake blending methods has been presented in reference [11] and [18]. It is the integrated control strategy during anti-lock braking that will be discussed here in this article.

5.1 The pneumatic anti-lock braking control strategy for a single wheel

Logic threshold method is the most widely used one. It monitors the accelerations of the wheels and estimates the vehicle speed. When the accelerations (decelerations) of the wheels reach the pre-set thresholds, the ABS takes particular measures, namely increase, hold or decrease the brake pressure, to keep the wheel slip within a range and maintain the longitudinal and lateral force between the wheels and the road surface. The thresholds of reference slip ratio act as assistance. Figure 4 illustrates the logic threshold method applied in a WABCO pneumatic ABS.

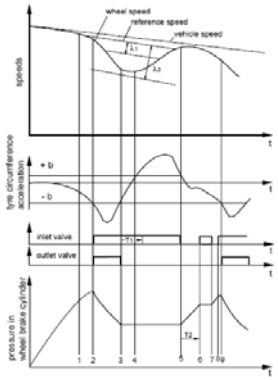

Figure 9 The logic threshold method applied in a WABCO pneumatic ABS[17]

Based on the revealed control strategies for pneumatic anti-lock braking, a control strategy for a single wheel is proposed here as the basis for integrated control, as shown in Fig.10.

The control of the pneumatic anti-lock braking is divided into 8 phases. The 8 phases cover the control on low friction, mid friction and high friction surfaces, indicating that in a single control cycle not every one of the phases is gone through. The 8 phases can be sorted as 'increase', 'hold' and 'decrease' meaning that in the according phase the brake pressure is increased, held or decreased. The thresholds used here include three rotational acceleration thresholds and two reference slip ratio thresholds, namely the deceleration threshold a_1 (used as $-a_1$), the lower acceleration threshold a_2, the higher acceleration threshold a_3, the lower slip ratio threshold s_1 and the higher slip ratio threshold s_2. All the thresholds mentioned above have positive value.

Phase 1 is a hold phase, which occurs when the deceleration of the wheel goes lower than $-a_1$. The control logic does not go into phase 2 as a decrease phase until the reference slip ratio reaches s_1 indicating that the wheel is at the edge of being locked, in order to keep the deceleration of the vehicle at a relatively high level. Phase 3 and phase 4 are twin-phases which are reached when the deceleration of the wheel decreases to be higher than $-a_1$. However phase 3 is a decrease phase occurring when the slip ratio is higher than s_2, while phase 4 is a hold phase occurring when the slip ratio is lower than s_2. When the friction parameter of the road surface is low the rotational speed of the wheel is regained slower than on a high friction surface. Phase 3 is to lower the slip ratio more actively on this condition keeping the wheel slip within control. Phase 5 is a hold phase, which can be seen as an extension of phase 4 on good friction condition when the acceleration of the wheel goes higher than a_2. On extremely good road surfaces as dry and clean asphalt, the acceleration of the wheel may reach a high level over a_3, which may decrease the slip ratio too quickly and make the brake force much lower than expected. Then phase 6 occurs to increase the brake pressure. Phase 7 acts as phase 5 when the formerly higher than a_3 acceleration gets back between a_2 and a_3. Phase 8 is an increase phase occurring when the acceleration is lower than a_2 indicating a small difference between the tangential speed of the wheel and the speed of the vehicle. When the wheel begins to decelerate and the deceleration is lower than $-a_1$ again, phase 2 occurs and a new control cycle commences. Note that phase 1 appears only in the very first control cycle.

Thus, on a low friction surface, a control cycle as (1)-2-3-4-5-8 is more likely to occur. On a medium friction surface, a control cycle as (1)-2-4-5-8 is more likely to occur. On a high friction surface, a

control cycle as (1)-2-4-5-6-7-8 is more likely to occur. It is also possible that phase 6 occurs on a low friction surface and phase 3 occurs on a high friction surface due to the complex relations among the vehicle, the wheels and the road surface.

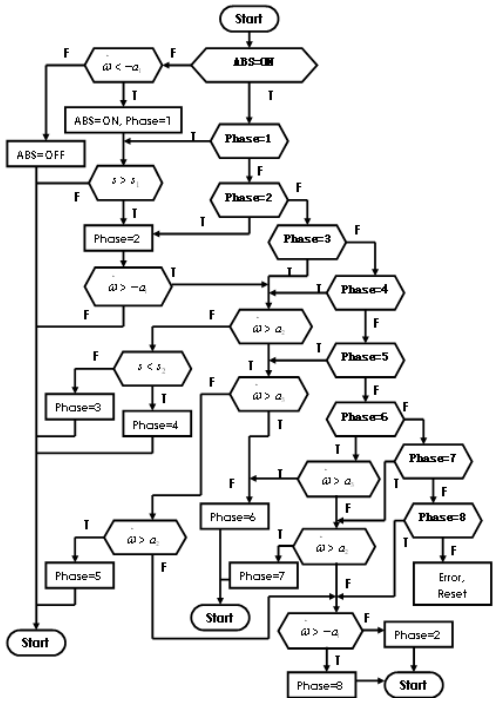

Figure 10. The control strategy for pneumatic anti-lock braking

5.2 The integrated anti-lock braking control strategy for drive wheels

The integrated anti-lock braking control strategy is for the two rear drive wheels connected to an electric motor via a final drive.

The control strategy for the pneumatic anti-lock braking is the same as in Figure 10. The braking torque by the electric motor is assumed to be shared equally between the two wheels. Thus the control strategy for the regenerative anti-lock braking should take the conditions of both wheels into consideration as shown in Figure11. The rotational acceleration of the left rear wheel is denoted as $\dot{\omega}_f$ and the slip ratio as s_f. Those of the right rear wheel are denoted as $\dot{\omega}_r$ and s_r.

The thresholds for both wheels are the same. The significations of the phases in the regenerative anti-lock braking control are the same as those in the pneumatic anti-lock braking control. The motor torque is limited by the parameter of itself and the capacity of the battery.

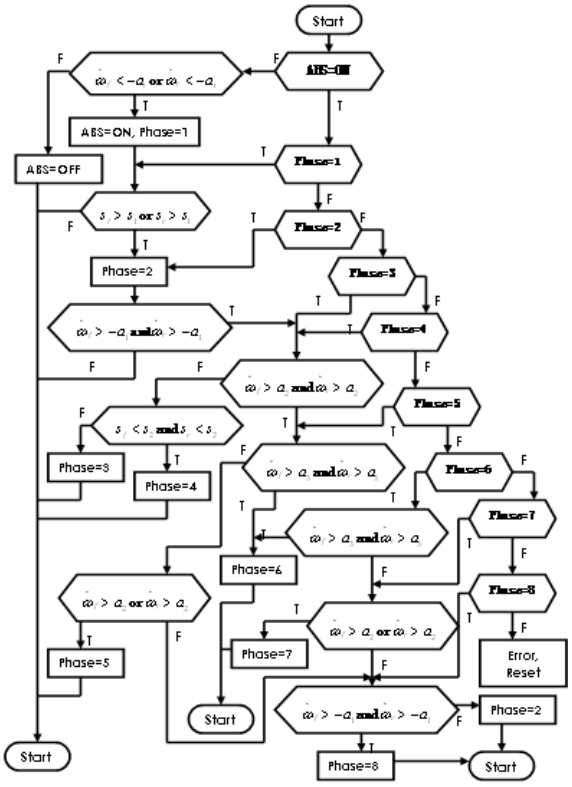

Figure 11. The control strategy for regenerative anti-lock braking of rear wheels

6 Simulation and hardware-in-the-loop control

6.1 Simulation

To evaluate the effect of the integrated control strategy during anti-lock braking, some simulations are carried out in MATLAB/Simulink. The subsystems of the model have been mentioned in part3.

The scenario for simulation is as follows: with initial speed of 80km/h, the brake is fully employed triggering the lock of wheels. As the highest deceleration possible for the HCNG hybrid bus is approximately 0.6g($\approx$6m/s^2), the surfaces used in the simulation are gravel surface (with a peak equivalent friction parameter of 0.614 and a sliding equivalent friction parameter of 0.557) and hard-packed snow surface (with a peak equivalent friction parameter of 0.216 and a sliding equivalent friction parameter of 0.136) ensuring that at least wheels of one axle may be locked.

The pneumatic anti-lock braking strategy is first verified. Note that in the anti-lock braking strategy the vehicle speed is estimated from the speed of

wheels, thus a difference between the actual speed of vehicle and the estimated speed can be expected. The difference is proved to be within tolerance of the control logic, as shown in Fig.12. The thresholds for slip ratio also take that into consideration.

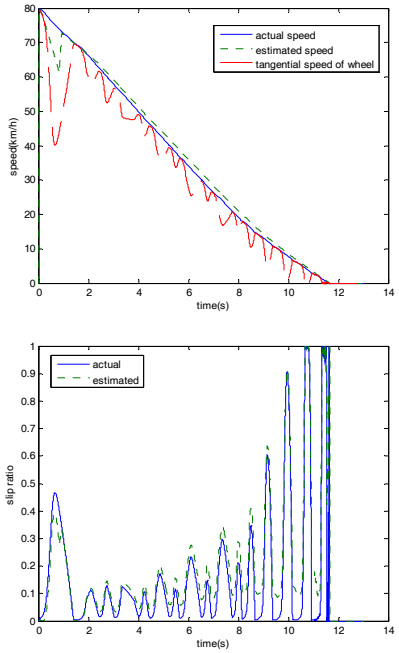

Figure 12. Estimated vehicle speed and estimated slip ratio

The tangential speed of the rear left wheel is also shown in Figure 12. The speed of the wheel is modulated properly and no lock is occurred. It is notable that at the beginning of the braking the speed of wheel drops abruptly. It is due to the inaccuracy of the estimated vehicle speed for the time being and the entrance logic of anti-locking braking (namely phase 1 of the strategy). The other three wheels are not locked as well.

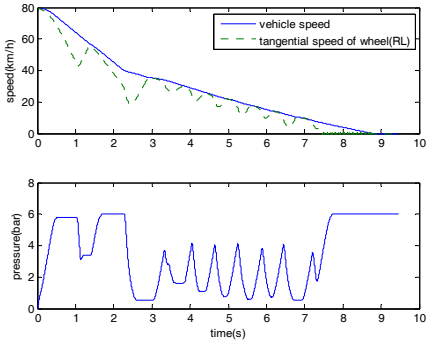

Figure 13 Result of jump- μ surface simulation, pneumatic anti-lock braking

Figure 13 illustrates the simulation of pneumatic anti-lock braking strategy on a jump- μ surface. On the medium friction surface the wheel begins to show sign of lock and then regains its speed due to modulation of anti-lock braking. The wheel moves on to the low friction surface and is near to be unstable for a while. Shortly after that the wheel is under the control of anti-lock braking periodically and is not locked. The brake of other three wheels is also modulated properly to avoid any wheel lock. The pneumatic anti-lock braking strategy has been proved to be effective. The integrated anti-lock braking strategy is simulated following the same procedure to make a comparison. The initial state of charge (SOC) of the battery is set to be 0.3. Figure 14 illustrates the result of simulation. It is notable that the fluctuation of the wheel speed is smoothed by modulating the motor torque. The pneumatic pressure is also decreased evidently. The result of jump- μ surface simulation is shown in Figure 15. The wheel speed is modulated properly as well. In no cases is a single wheel locked.

The results from the simulation on low friction surface of the pneumatic anti-lock braking and that of the integrated anti-lock braking are compared specifically in Table 2.

Table 2 Comparison of pneumatic anti-lock braking and integrated anti-lock braking

	Pneumatic anti-lock braking	Integrated anti-lock braking
Average deceleration (m/s^2)	-2.00	-2.04
Average jerk (m/s^3)	3.36	2.88
Average pneumatic pressure (bar)	2.00	1.39
Energy regenerated (KJ)	-	14.1
80~0km/h Displacement (m)	120.2	117.4

Although the stopping distances and the average decelerations for both kinds of anti-lock braking are almost the same, the integrated anti-lock braking decrease the fluctuation of the vehicle acceleration effectively. The pneumatic pressure needed by the pneumatic brake during anti-lock braking is also much lower. Thus integrated anti-lock braking not only ensures a better ride for passengers, but also a quicker response of the pneumatic brake, considering that the inflation of the brake chamber diaphragm may be agiler when the pressure gap between air reservoir and the brake chamber is bigger.

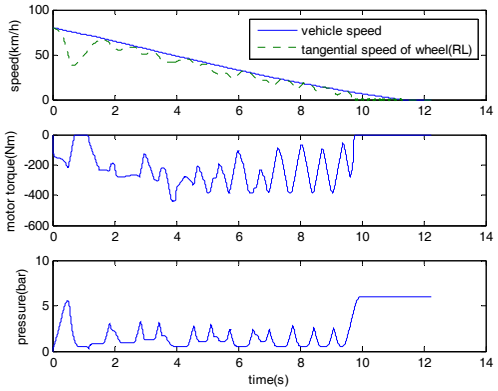

Figure 14 Result of low friction surface simulation, integrated anti-lock braking

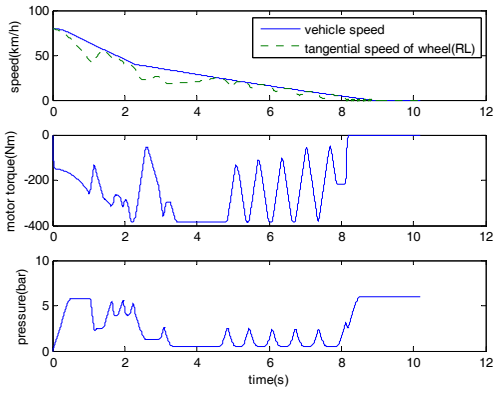

Figure 15 Result of jump- μ surface simulation, integrated anti-lock braking

6.2 Hardware-in-the-loop test

The pneumatic anti-lock braking strategy is test first on the test bench. The result is shown in Fig.15. The actual pneumatic pressure fluctuation is more tempestuously than that in the simulation. The wheel speed drops also deeper than in the simulation. The overall effect of anti-lock braking control is good. No wheel is lock during deceleration.

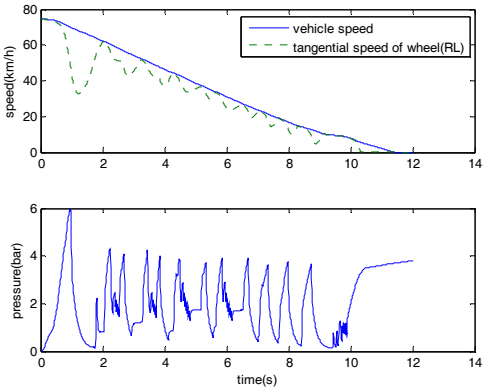

Figure 15 Result of low friction surface HIL test, pneumatic anti-lock braking

The test result of integrated anti-lock braking control is illustrated in Fig.16. The pattern of wheel speed fluctuation resembles that under pneumatic anti-lock braking. The way pneumatic pressure is modulated is more moderate.

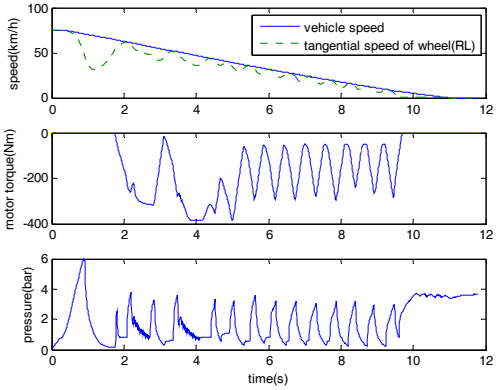

Figure 16 Result of low friction surface HIL test, integrated anti-lock braking

A jump- μ surface HIL test is also carried out under integrated anti-lock braking. The result is illustrated in Fig.17 and Fig.18. No rear wheel is locked in the test. Although the front wheels are lock at the moment of μ -jump as shown in Fig.18, the speeds of wheels are regained very quickly. Thus the stability of vehicle is still maintained during deceleration.

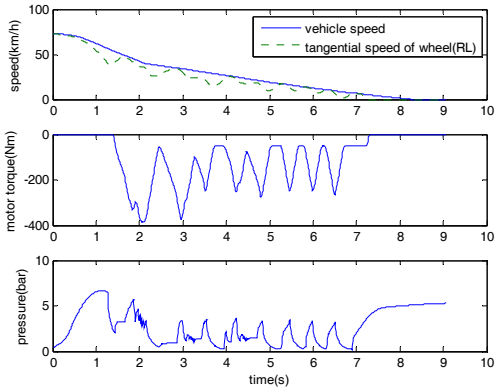

Figure 17 Result of jump- μ surface HIL test, integrated anti-lock braking

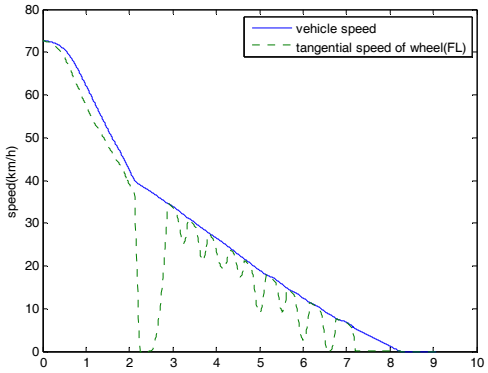

Figure 18 Result of jump- μ surface HIL test, integrated anti-lock braking, left front wheel

Comparing with pneumatic anti-lock braking based on HIL test results, the integrated anti-lock braking is still advantageous in the ride of vehicle and the agility of pneumatic pressure. For example, the average jerk is 3.349m/s^3 under pneumatic control and that under integrated control is 3.123 m/s^3. The average pneumatic pressure under pneumatic control is 1.9bar and that under integrated control is 1.6bar.

7 Conclusion

Based on a series regenerative braking system an integrated brake system combining the regenerative braking of the electric motor and the friction braking of the pneumatic brakes is proposed. The system employs the same set of valves to modulate the pneumatic pressure during brake blending and anti-lock braking control. The control strategy is proposed for the anti-lock braking control of the friction braking and regenerative braking. Simulations are carried out on authorized models. Hardware-in-the-loop tests are carried out on a test bench featuring the pneumatic brake system of a common bus.

The results of simulation and HIL tests show that the integrated anti-lock braking control is advantageous in riding comfort and quick response of the pneumatic system. It also ensures the stability and safety of the vehicle. At the mean time a fraction of braking energy can be regenerated.

Further study could be carried out on the influence of anti-lock regenerative braking on the power-train, the optimization of the integrated control strategy and the influence of integrated anti-lock braking on lateral stability of vehicle.

References

[1] Yinmin Gao, Liping Chen, Mehrdad Ehsani. *Investigation of the Effectiveness of Regenerative Braking for EV and HEV*. SAE International SP-1466. 1999-01-2910. 1999.

[2] Mehrdad Ehsani, Yimin Gao, Karen L Butler. *Application of Electrically Peaking Hybrid (ELPH) Propulsion System To A Full Size Passenger Car With Simulated Design Verification.* IEEE Transaction On Vehicular Technology. Vol.48, No.6, Nov. 1999.

[3] *Hybrid check list: What kind of Hybrid is it?* http://www.hybridcenter.org, accessed on 2009-03-06

[4] Michael Panagiotidis, George Delagrammatikas, Dennis Assanis. *Development and Use of a Regenerative Braking Model for a Parallel Hybrid Electric Vehicle*, SAE Paper 2000-01-0995. SAE World Congress, Detroit, MI, 2000.

[5] J. Pickenhahn, L. Gilles, Th. Hönig, P. Thomas. *Concepts for Regenerative Braking in Vehicles with Hybrid Propulsion Drive*, XXVIth International μ Symposium.

[6] *In the Autoblog Green Garage: 2008 Honda Civic* Hybrid.http://www.autobloggreen.com accessed on 2009-03-06

[7] Wade D. Bartlett. *Calculation of Deceleration Rates for S-Cam Air-Braked Heavy Trucks Equipped withAnti-Lock Brake Systems.* SAE International SP-2063. 2007-01-0714. 2007.

[8] Akihito Kusano, *Brake Pressure Control Device for Automotive Vehicles*, U.S. Patent, 2000

[9] Wolfgang Fey, Georg Fachinger, Mario Engelmann, etc., *Electrohydraulic Brake System*, U.S. Patent, 2001

[10] Kazuhiro Tagata, Koji Sakai, Yasushi Aoki, etc., *Vehicle Brake Device*, U.S. Patent, 2007

[11] Zhang, Junzhi; Lu, Xin; Zhang, Pengjun; Chen, Xin. *Road test of hybrid electric bus with regenerative braking system*, Jixie Gongcheng Xuebao/Journal of Mechanical Engineering, ISSN1000-9345, v 45, n 2, p 25-30, February 2009.

[12] Chu Liang, etc., *Pneumatic Anti-lock braking system for hybrid commercial vehicles*, Chinese Patent, application number: 200610017245.0, 2007

[13] Gim.G and Nikravesh.P.E.(1990). *An analytical model of pneumatic tyres for vehicle dynamic simulations. Part 1: Pure slips.* Int. J. of Vehicle Design, ISSN (printed): 0143-3369, vol. 11. No. 6, pp. 589-618

[14] Gim.G and Nikravesh.P.E.(1991). *An analytical model of pneumatic tyres for vehicle dynamic simulations. Part 3: Validation against experimental data.* Int. J. of Vehicle Design, ISSN (printed): 0143-3369, vol. 12. No. 2, pp. 217-228

[15] Bohm F. *Mechanik des.Gurtelreifens.*Ingenieur- Archiv. 1966 (35) : 82～101

[16] Subramanian, Shankar C.; Darbha, Swaroop; Rajagopal, K.R. *Modeling the pneumatic subsystem of an s-cam air brake system. Journal of Dynamic Systems*, Measurement and Control, Transactions of the ASME, v 126, n 1, p 36-46, 2004

[17] *ABS/ASR „D"-„Cab" – Version Anti-Lock Braking System for Commercial Vehicles*, 1st edition, WABCO, 2006

[18] Zhang Junzhi, Lu Xin, Chen Shanglou, Zhang Pengjun. *Coordinated control for regenerative braking system.* Vehicle Power and Propulsion Conference, 2008. VPPC '08. IEEE 3-5 Sept. 2008 Page(s):1 - *6*

Authors

Junzhi Zhang, Professor, State Key Laboratory of Automotive Safety and Energy , Tsinghua University, Beijing, China. Research Interests: Automotive Hybrid Powertrain. Current Research, Optimization of hybrid powertrain, Energy management of hybrid powertrain, Control and test of hybrid powertrain.